PORTIONS OF THIS DOCUMENT ARE ILLEGIBLE

LA-UR -82-1045

CONF-820429--7

Los Alamos National Laboratory is operated by the University of California for the United States Department of Energy under contract W-7405-ENG-36.

LA-UR--82-1045

DE82 014047

TITLE: SOLUTION OF THE FOKKER-PLANCK EQUATION FOR CHARGED-PARTICLE TRANSPORT IN ONE SPACE DIMENSION

AUTHOR(S): Thomas A. Oliphant and Antonio Andrade

SUBMITTED TO Los Alamos/CEA Applied Physics Conference, Paris, France, April 19-23, 1982

Los Alamos Los Alamos National Laboratory
Los Alamos, New Mexico 87545

FORM NO 836 R4
ST NO 2629 5/81

SOLUTION OF THE FOKKER-PLANCK EQUATION FOR CHARGED PARTICLE TRANSPORT IN ONE SPACE DIMENSION

Thomas A. Oliphant and Antonio Andrade
Los Alamos National Laboratory
Los Alamos, New Mexico

ABSTRACT

In the study of charged particle transport in plasmas, numerical techniques for solving the Fokker-Planck equation have been developed which closely parallel those used in neutron transport. This was a natural step since the theory and methods of neutron transport have been well developed. Moreover a line of treatment has been developed tailored to the specific requirements of transport in mirror machines. This approach involves the assumption that the distribution function remain constant along a guiding center orbit. Diffusion techniques have been developed in which sequential moments of the transport equation are taken so as to generate a set of coupled equations. Here a method is developed which treats the transport operator according to the standard diamond differencing techniques of neutron transport, but treats the collision term by a method designed to take advantage of the form of the Fokker-Planck collision operator. This latter method makes use of matrix factorization techniques. In the absence of applied external fields, this method conserves particles rigorously. Deterministic methods run into difficulty in the treatment of magnetized plasmas in cases in which the guiding-center approximation does not apply. Thus, there are some situations in which one is driven to Monte Carlo techniques which are not a subject of this paper.

I. INTRODUCTION

In the study of charged particle transport in plasmas, numerical techniques for solving the Fokker-Planck equation have been developed which closely parallel those used in neutron transport. This was a natural step in the development of solution methods in charged particle transport (CPT) in view of the fact that the theory and methods of neutron transport have been well developed[1,2]. Moreover, since much of the pioneering work in CPT was carried out in conjunction with the on-going effort to build controlled fusion devices, the early methodologies developed to solve the transport equation were made more applicable to those machines. In the well known analysis of transport in mirror machines by Killeen, et al[3] for example, the calculations of spatial changes along the magnetic field are based on an assumption that the distribution function of ions remain approximately constant along a guiding center orbit; an assumption which is sufficiently accurate and more appropriate for low density mirror confinement systems.

Other authors have used expansion methods[4,5] or diffusion theory techniques[6] to solve the transport equation. The diffusion techniques require that sequential moments of the transport equation be taken so as to generate a coupled set of equations, and further require that a prescription for closing that set be given. The transport problem is then reduced to the solution of that set.

In other methods[7,8], the differencing and multigrouping techniques of neutronics are directly applied to yield solutions to the CPT equation by standard algorithms. In all of the methods mentioned above however, the Fokker-Planck collision term is usually approximated in some fashion. The diffusion techniques, for example, usually include only a treatment of collisional slowing down without velocity space dispersion ("straight-line slowing down"). The S_n techniques of Ref. 7 are also applied to a Boltzmann-like equation in which only straight-line slowing down is considered in a deceleration term. As will be discussed in this presentation the exclusion of velocity space dispersion may lead to very inaccurate results.

Recently, some researchers have attempted to solve the Fokker-Planck (FP) equation without recourse to approximations. This was done by either reformulating the FP collision term into a form which matches the structure of a standard neutronics code[9] such that existing computer programs can be used directly for CPT, or by deriving cross sections[10] which simulate the slowing down of ions to be used in existing neutronics codes. The drawbacks that were found to these approaches were that the large computer codes were cumbersome to modify or as in the case of Ref. 9, the existing code structure forced a semi-implicit differencing of the collision term which subsequently led to long computer runs.

More recently a method has been developed to solve the Fokker-Planck charged particle transport equation by simple and efficient means, and without approximation to the collision term[11]. In this method the kinetic equation is integrated to yield the time dependent distribution function of test particles $f_a(r,v,t)$ in a fully implicit manner by a combination of S_n methodology with a matrix factorization technique. The full three dimensional velocity space dependence along with the radial configuration space dependence of the distribution function is obtained as a function of time by this method if all of the phase space variables are treated as discrete. This latter method is the primary object of discussion in the text that follows. More details may be found in the dissertation of A. Andrade[12].

Although the method discussed below can be applied to cylindrically symmetric problems, the essential ideas are contained in the spherically symmetric case which is the only one to be considered in this text.

II. THE FOKKER-PLANCK TRANSPORT EQUATION

The kinetic equation which characterizes the transport of charged particles in a plasma as they suffer collisions which result in their deflection by small angles has come to be known as the Fokker-Planck transport equation and is given by

$$\frac{\partial f_a(\underline{r},\underline{v},t)}{\partial t} + \underline{v} \cdot \frac{\partial f_a}{\partial \underline{r}} + \frac{\underline{F}^{ext}}{m_a} \cdot \frac{\partial f_a}{\partial \underline{v}} - \frac{1}{m_a} \frac{\partial \langle \phi \rangle}{\partial \underline{r}} \cdot \frac{\partial f_a}{\partial \underline{v}} = \frac{\partial f_a}{\partial t}\Big)_c \qquad (2\text{-}1)$$

where

$$\frac{\partial f_a}{\partial t}\Big)_c = -\sum_b \{\nabla_{\underline{v}} \cdot (f_a \langle \Delta \underline{v} \rangle) - \frac{1}{2} \nabla_{\underline{v}} \nabla_{\underline{v}} : (f_a \langle \Delta \underline{v} \Delta \underline{v} \rangle)\} \qquad (2\text{-}2)$$

is the collision term of the equation. $\langle \phi \rangle$ is the average electrostatic potential at $\underline{r}$ produced by the particles at other positions while $\underline{F}^{ext}$ is the force experienced by the plasma particles at $\underline{r}$ due to externally applied electromagnetic fields. Eq. (2-1), therefore is an equation for the time evolution of the one particle distribution function of particles of species 'a', as this distribution is affected by internal and external forces and as it is affected by collisions with plasma particles of all species 'b' within a given system, including collisions among its own species 'a'.

Rosenbluth, MacDonald, and Judd[13] first formulated the averages $\langle \Delta v \rangle$ and $\langle \Delta v \Delta v \rangle$ in Eq. (2-2) in terms of the potential-like functions $h_{ab}(v)$ and $g_{ab}(v)$ as

$$\langle \Delta \underline{v} \rangle = \Gamma_{ab} \nabla_{\underline{v}} h_{ab}(\underline{v}) \tag{2-3}$$

$$\langle \Delta \underline{v} \Delta \underline{v} \rangle = \Gamma_{ab} \nabla_{\underline{v}} \nabla_{\underline{v}} g_{ab}(\underline{v}) \tag{2-4}$$

where

$$h_{ab}(\underline{v}) = \frac{A_a + A_b}{A_b} Z_b^2 \int d\underline{u}\ f_b(\underline{r},\underline{u},t) \left|\underline{v}-\underline{u}\right|^{-1} \tag{2-5}$$

and

$$g_{ab}(\underline{v}) = Z_b^2 \int d\underline{u}\ f_b(\underline{r},\underline{u},t) \left|\underline{v}-\underline{u}\right|. \tag{2-6}$$

Here $\Gamma_{ab} = (Z_a^2 e^4 / 4\pi m_a^2 \varepsilon_o^2) \ln\Lambda$ and $\ln\Lambda = \ln(\lambda_d / b_o)$ where λ_d is the Debye length $[\sum_b n_b Z_b e^2 / kT_b \varepsilon_o]^{-1/2}$ and b_o is the impact parameter for scattering at 90° which is equal to $Z_a Z_b e^2 / 4\pi\varepsilon_o \mu_{ab} V^2$. Defining the integrals in Eqs. (2-5) and (2-6) as

$$L_b(\underline{v}) = \int d\underline{u}\ f_b(\underline{r},\underline{u},t) \left|\underline{v}-\underline{u}\right|^{-1} \tag{2-7}$$

$$K_b(\underline{v}) = \int d\underline{u}\ f_b(\underline{r},\underline{u},t) \left|\underline{v}-\underline{u}\right| \tag{2-8}$$

the potential-like relationship between Eqs. (2-5) and (2-6) is easily shown with

$$\nabla_{\underline{v}}^2 K_b(\underline{v}) = 2 L_b(\underline{v}) \tag{2-9}$$

and

$$\nabla_{\underline{v}}^2 L_b(\underline{v}) = -4\pi f_b(\underline{r},\underline{v},t). \tag{2-10}$$

In this presentation, the effects of internal and external forces on the evolution of f_a will not be considered so that $\langle \phi \rangle$ and $\underline{F}^{ext}$ in Eq. (2-1) can effectively be set equal to zero.

III. SPHERICAL SYMMETRY IN CONFIGURATION SPACE

A symmetric, field-free, spherical plasma configuration is a particularly simple system in which new techniques for solving the transport equation can be tested. Since results of benchmark calculations in this type of system exist in abundance, comparisons can easily be made.

To this end, consider the time evolution of a distribution $f_a(r,v,\mu,t)$ of test particles in a fully symmetric state in a spherical configuration space and in a spherical velocity space in which the distribution function will only be constrained to be azimuthally symmetric. In this case the transport equation is written as

$$\frac{\partial f_a(r,v,\mu,t)}{\partial t} + \frac{v\mu}{r^2}\frac{\partial}{\partial r}(r^2 f_a) + \frac{v\partial}{r\partial\mu}[(1-\mu^2)f_a] = \frac{\partial f_a}{\partial t}\Big)_c \tag{3-1}$$

where

$$\frac{\partial f_a}{\partial t}\Big)_c = -\{\frac{1}{v^2}\frac{\partial}{\partial v} v^2 J^v + \frac{\partial}{\partial \mu} J^\mu\} \tag{3-2}$$

and

$$J^v = \sum_b \Gamma_{ab} \frac{N_o \tau_o}{C_o^3} Z_b^2 \{\frac{A_a}{A_b} f_a \frac{\partial L_b}{\partial v} - \frac{1}{2}[\frac{\partial f_a}{\partial v}\frac{\partial^2 K_b}{\partial v^2}]\} \tag{3-3}$$

$$J^\mu = \sum_b \Gamma_{ab} \frac{N_o \tau_o}{C_o^3} Z_b^2 \{-\frac{(1-\mu^2)}{2v^2}[\frac{1}{v}\frac{\partial f_a}{\partial \mu}\frac{\partial K_b}{\partial v}]\}. \tag{3-4}$$

In the above equations and in the remainder of this work dimensionless variables are used which are defined as follows

$$n = \frac{n}{N_o} \quad v = \frac{v}{C_o} \quad t = \frac{t}{\tau_o}$$

where N_o and τ_o are chosen to suit the problem at hand and where C_o is defined to be $(2kT_o/m_o)^{1/2}$. K is Boltzmann's constant, T_o is a standard kinetic temperature and m_o is the mass corresponding to 1 AMU. With these scalings the scaled distribution function is related to the unscaled distribution by

$$\tilde{f} = fC_o^3/n_o.$$

it is found that the Fokker-Planck transport equation retains its original form if the traditional Γ_{ab} is replaced by $\Gamma_{ab}N_o\tau_o/C_o^3$. In equations (3-1) through (3-4) the tildes have been dropped for brevity. Here the functions K_b and L_b of the background distributions f_b will remain isotropic for all time and the sums over the species 'b' will not include the species 'a' so that the treatment of Eq. (3-1) will become fully linear. The background Maxwellian distribution functions in scaled variables have the form

$$f_b(u) = \frac{n_b}{\pi^{3/2} v_{ob}^3} \exp(-u^2/v_{ob}^2) \tag{3-5}$$

where $v_{ob} = (T_b/A_b)^{1/2}$.

With the definitions of K_b and L_b given by Eqs. (2-7) and (2-8), the derivatives in J^v and J^u can be computed as

$$\frac{\partial L_b}{\partial v} = -\frac{4\pi}{v^2}\int_0^v u^2 f_b(u)du \tag{3-6}$$

$$\frac{\partial K_b}{\partial v} = 4\pi\int_0^v (u^2 - \frac{u^4}{3v^2}) f_b(u)du + 4\pi\int_v^\infty \frac{2uv}{3} f_b(u)du \tag{3-7}$$

$$\frac{\partial^2 K_b}{\partial v^2} = 4\pi\int_0^v \frac{2u^4}{3v^3} f_b(u)du + 4\pi\int_v^\infty \frac{2}{3} u f_b(u)du. \tag{3-8}$$

Defining the standard integrals in Eqs. (3-6) - (3-8) as

$$H_{b1}(v) = \int_v^\infty u f_b du \tag{3-9}$$

$$H_{b2}(v) = \int_0^v u^2 f_b du \tag{3-10}$$

$$H_{b3}(v) = \int_0^v u^4 f_b du, \tag{3-11}$$

it is seen that the Landau-Fokker-Planck components can then be rewritten as

$$J^v = -4\pi \sum_b \Gamma_{ab} \frac{N_o \tau_o}{C_o^3} Z_b^2 \{ \frac{A_a}{A_b} f_a \frac{H_{b2}(v)}{v^2} + \frac{1}{3} \frac{\partial f_a}{\partial v} \left(\frac{H_{b3}(v)}{v^3} + H_{b1}(v) \right) \} \tag{3-12}$$

and

$$J^\mu = -4\pi \sum_b \Gamma_{ab} \frac{N_o \tau_o}{C_o^3} Z_b^2 \{ \frac{(1-\mu^2)}{2v^3} \frac{\partial f_a}{\partial \mu} \times \left(H_{b2}(v) - \frac{H_{b3}(v)}{3v^2} + \frac{2v}{3} H_{b1}(v) \right) \} \tag{3-13}$$

Since the background distributions are Maxwellian, the integrals H_{b1}, H_{b2}, and H_{b3} are easily evaluated as

$$H_{b1}(v) = \frac{n_b}{2\pi^{3/2} v_{ob}} \exp(-v^2/v_{ob}^2) \tag{3-14}$$

$$H_{b2}(v) = \frac{n_b}{\pi^{3/2}} \left[\frac{\pi^{1/2}}{4} \operatorname{erf}(v/v_{ob}) - \frac{v}{2v_{ob}} \exp(-v^2/v_{ob}^2) \right] \tag{3-15}$$

$$H_{b3}(v) = \frac{n_b v_{ob}^2}{2\pi^{3/2}} \left[\frac{3\pi^{1/2}}{4} \operatorname{erf}(v/v_{ob}) - \right.$$

$$\left. \frac{v}{v_{ob}} \left(\frac{3}{2} + \frac{v^2}{v_{ob}^2}\right) \exp(-v^2/v_{ob}^2)\right]. \tag{3-16}$$

Equation (3-1) can be solved by a direct finite difference method which is similar in many respects to the S_n technique used in neutron transport. In this method the angular dependence of the distribution function is not expanded via a complete set of functions but rather is treated as discrete. The way in which the methodology presented in this chapter varies from the standard S_n method is in the treatment of the collision physics. Here the collision effects will be solved for separately from the streaming effects.

An operator κ which will descretize all of the arguments of $f_a(r,v,\mu,t)$ through the transport equation is

$$\kappa = \frac{1}{\beta}\int_{t_s}^{t_{s+1}} dt \int_{r_{i-1/2}}^{r_{i+1/2}} r^2 dr \int_{v_{g-1/2}}^{v_{g+1/2}} v^2 dv \int_{\mu_{n-1/2}}^{\mu_{n+1/2}} d\mu \tag{3-17}$$

where $\beta = \Delta t_s(\Delta r_i^3/3)(\Delta v_g^3/3)\Delta\mu_n$ and $\Delta t_s = t_{s+1} - t_s$, $\Delta r_i^3/3 = (r_{i+/2} - r_{i-1/2}^3)/3$, $\Delta v_g^3/3 = (v_{g+1/2}^3 - v_{g-1/2}^3)/3$, $\Delta\mu_n = \mu_{n+1/2} - \mu_{n-1/2}$.

In this analysis the intervals on a mesh will be centered at integer values of the indices s,i,g and n and the distribution function f_a will always be defined at $t = t_{s+1}$ i.e., implicitly, unless specified by a subscript to be otherwise.

Applying the operator κ to Eq. (3-1) yields the difference approximation

$$\frac{f(r_i, v_g, \mu_n, t_{s+1}) - f_s}{\Delta t_s} + \frac{\mu_n \Delta v_g^4/4}{V_i \Delta v_g^3/3} [A_{i+1/2} f_{i+1/2} -$$

$$A_{i-1/2} f_{i-1/2}] + \frac{\Delta v_g^4/4}{V_i \Delta \mu_n \Delta v_g^3/3} [\alpha_{n+1/2} f_{n+1/2} - \alpha_{n-1/2} f_{n-1/2}]$$

$$= -\{ \frac{1}{\Delta v_g^3/3} [v^2_{g+1/2} J^v_{g+1/2} - v^2_{g-1/2} J^v_{g-1/2}] + \tag{3-18}$$

$$\frac{1}{\Delta \mu_n} [J^\mu_{n+1/2} - J^\mu_{n-1/2}]\}$$

where $V_i = \Delta r_i^3/3$, $A_{i+1/2} = r^2_{i+1/2}$, and where the angular streaming term has been differenced as in the S_n methodology of neutronics[14] in order to preserve conservation of particles for finite sized intervals $\Delta \mu_n$. The subscript 'a' of the test distribution has been dropped since it is understood that this is an equation for f_a.

By using the definitions

$$R_g = A_a \sum_b \Gamma_{ab} \frac{N_o \tau_o Z_b^2}{C_o^3 A_b} H_{b2}(v_g) \tag{3-19}$$

$$C_g = \frac{1}{3} \sum_b \Gamma_{ab} \frac{N_o \tau_o}{C_o^3} Z_b^2 \left(\frac{H_{b3}(v_g)}{v_g} + v_g^2 H_{b1}(v_g) \right) \tag{3-20}$$

$$D_g = \sum_b \Gamma_{ab} \frac{N_o \tau_o Z_b^2}{C_o^3 v_g^3} \left(H_{b2}(v_g) - \frac{1}{3v_g^2} H_{b3}(v_g) + \frac{2}{3} v_g H_{b1}(v_g) \right) \tag{3-21}$$

in Eqs. (3-12) and (3-13), the components of $\underline{J}$ in the collision term of the difference approximation become

$$J^v_{g+1/2} = -\frac{4\pi}{v^2_{g+1/2}} \{ B_{g+1/2} f_{g+1/2} + C_{g+1/2} \left(\frac{f_{g+1} - f_g}{\Delta v_{g+1/2}} \right) \} \tag{3-22}$$

$$J^{v}_{g-1/2} = -\frac{4\pi}{v^{2}_{g-1/2}}\{B_{g-1/2} f_{g-1/2} + C_{g-1/2}\left(\frac{f_{g} - f_{g-1}}{\Delta v_{g-1/2}}\right)\} \tag{3-23}$$

$$J^{\mu}_{n+1/2} = -2\pi D_{g}\{(1-\mu^{2}_{n+1/2}) \frac{f_{n+1/2} - f_{n}}{\Delta \mu_{n+1/2}} \tag{3-24}$$

$$J^{\mu}_{n-1/2} = -2\pi D_{g}\{(1-\mu^{2}_{n-1/2}) \frac{f_{n} - f_{n-1}}{\Delta \mu_{n-1/2}} \tag{3-25}$$

The velocity grid interval edge values $f_{g\pm1/2}$ in the $J^{v}_{g\pm1/2}$ components can be related to the centered values f_{g} by the interpolating relations of Chang and Cooper[15] as

$$f_{g+1/2} = (1 - \delta_{g+1/2}) f_{g+1} + \delta_{g+1/2}\, f_{g} \tag{3-26}$$

$$f_{g-1/2} = (1 - \delta_{g-1/2}) f_{g} + \delta_{g-1/2}\, f_{g-1} \tag{3-27}$$

where

$$\delta_{g\pm1/2} = \frac{1}{\omega_{g\pm1/2}} - \frac{1}{[\exp(\omega_{g\pm1/2}) - 1]} \tag{3-28}$$

and

$$\omega_{g\pm1/2} = \frac{\Delta v_{g} B_{g+1/2}}{D_{g\pm1/2}} \tag{3-29}$$

By using these relations in Eqs. (3-22) and (3-23), the collision term of Eq. (3-18) can be rewritten as the sum of two terms as

$$\tilde{q} = \tilde{q}^{v} + \tilde{q}^{\mu} \tag{3-30}$$

where

$$\tilde{q}^{v} = \frac{4\pi}{\Delta_g^3/3}\{f_{g-1}[\frac{C_{g-1/2}}{\Delta v_{g-1/2}} - B_{g-1/2}\delta_{g-1/2}]$$

$$+f_g[B_{g+1/2}\delta_{g+1/2} - B_{g-1/2}(1 - \delta_{g-1/2}) - \frac{C_{g-1/2}}{\Delta v_{g-1/2}} - \frac{C_{g+1/2}}{\Delta v_{g+1/2}}]$$

$$+ f_{g+1}[B_{g+1/2}(1 - \delta_{g+1/2}) + \frac{C_{g+1/2}}{\Delta v_{g+1/2}}]\} \qquad (3\text{-}31)$$

and

$$\tilde{q}^{\mu} = \frac{2\pi}{\Delta\mu_n} D_g\{f_{n-1}\frac{(1 - \mu^2_{n-1/2})}{\Delta\mu_{n-1/2}}$$

$$- f_n[\frac{(1 - \mu^2_{n+1/2})}{\Delta\mu_{n+1/2}} + \frac{(1 - \mu^2_{n-1/2})}{\Delta\mu_{n-1/2}}]$$

$$+ f_{n+1}\frac{(1 - \mu^2_{n+1/2})}{\Delta\mu_{n+1/2}}\} \qquad (3\text{-}32)$$

Note that $\tilde{q}$ is a sum of two 3-point differnce terms.
By further defining the quantities

$$\xi = \frac{\Delta v_g^4/4}{V_i\Delta v_g^3/3} \qquad (3\text{-}33)$$

$$\Lambda = \mu_n\Delta\mu_n[A_{i+1/2}f_{i+1/2} - A_{i-1/2}f_{i-1/2}]$$

$$+ [\alpha_{n+1/2}f_{n+1/2} - \alpha_{n-1/2}f_{n-1/2}] \qquad (3\text{-}34)$$

and then combining Eqs. (3-30) and (3-18), it is seen that the transport equation can be written in the simple form

$$f - \bar{q}\Delta t_s = f_s - \frac{\xi\Lambda\Delta t_s}{\Delta\mu_n} \quad . \tag{3-35}$$

In this equation, it is seen that the collision terms are now on the L.H.S. while the streaming terms have been separated off into the R.H.S. This formulation suggests that a splitting procedure may be used to solve for the effects of collisions and streaming on the distribution separately and then combined in some self-consistent fashion to yield an updated distribution.

Eq. (3-35) can be split into two, separate, fully implicit equations of the fo.

$$[f - q\Delta t]^* = [f_s - \frac{\xi\Lambda\Delta t_s}{\Delta\mu_n}]_{t = t_s} \tag{3-36}$$

and

$$f + \frac{\xi\Lambda\Delta t_s}{\Delta\mu_n} = \bar{q}^*\Delta t_s + f_s. \tag{3-37}$$

Here Eq. (3-36) is seen to be an equation which modifies the distribution function f for collision effects while using the streaming terms as a constant known source term evaluated with quantities defined at the previous time step while Eq. (3-37) is an equation which corrects f for streaming and uses the result f* of Eq. (3-36) as $q^* = q(f^*)$ as a constant. When Eqs. (3-36) and (3-37) are solved together within a given time step, the distribution function $f(r_i, v_g, \mu_n, t_{s+1})$ is then determined for all i, g, and n.

Consider first Eq. (3-36) and recall that q was defined as the sum of two 3-point terms in Eqs. (3-30)-(3-32). As such, Eq. (3-36) resembles the differenced 2-dimensional Poisson equation which has the form

$$E_{ng}^{lk}\psi_{lk} + G_{ng}^{lk}\psi_{lk} = S_{ng} \tag{3-38}$$

$$l = n-1, n, n+1$$

$$k = g-1, g, g+1$$

where the matrices $\underline{\underline{E}}$ and $\underline{\underline{G}}$ contain the coefficients of the two 3-point terms q^{ν} and q^{μ} respectively and where S_{ng} corresponds to the source term on the R.H.S. of Eq. (3-36). E^{lk}_{ng} and G^{lk}_{ng} are actually supermatrices with the properties

$$E^{lk}_{ng} \rightarrow \delta^{l}_{n} E^{lk}_{ng} \tag{3-39}$$

$$G^{lk}_{ng} \rightarrow \delta^{k}_{g} G^{lk}_{ng} \tag{3-40}$$

where the first pair of upper and lower indeces indicate the position of an elemental matrix in the supermatrix and where the second pair indicate an element in the elemental matrices. Hence $\underline{\underline{E}}$ and $\underline{\underline{G}}$ have the forms

$$E^{lk}_{ng} = \begin{pmatrix} \begin{pmatrix} x & x & \\ x & x & x \\ & x & x \end{pmatrix}_{NGxNG} & & \\ & \begin{pmatrix} x & x & \\ x & x & x \\ & x & x \end{pmatrix} & \\ & & \begin{pmatrix} x & x & \\ x & x & x \\ & x & x \end{pmatrix} \end{pmatrix}_{NNxNN} \tag{3-41}$$

$$G^{lk}_{ng} = \begin{pmatrix} \begin{pmatrix} x & & \\ & x & \end{pmatrix}_{x} \begin{pmatrix} x & & \\ & x & \end{pmatrix}_{x} & & \\ & \begin{pmatrix} x & & \\ & x & \end{pmatrix}_{x} \begin{pmatrix} x & & \\ & x & \end{pmatrix}_{x} \begin{pmatrix} x & & \\ & x & \end{pmatrix}_{x} & \\ & & \begin{pmatrix} x & & \\ & x & \end{pmatrix}_{x} \begin{pmatrix} x & & \\ & x & \end{pmatrix}_{x} \end{pmatrix}_{NNxNN} \tag{3-42}$$

where NG is the number of intervals on the g grid and NN is the number of intervals on the n grid. The supervectors Ψ_{1k} and S_{ng} have the forms

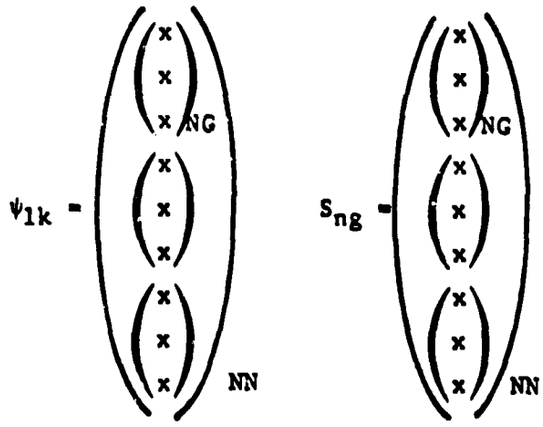

(3-43)

The notation of Eq. (3-38) can be simplified somewhat if the index g is taken to be vector index so that it can be rewritten as

$$\overleftrightarrow{E}\vec{\psi}_n + G_n^1\vec{\psi}_1 = \vec{S}_n \qquad (3\text{-}44)$$

This equation merely indicates that each multiplication of a superrow of Eqs. (3-41) and (3-42), by a supercolumn of $\vec{\Psi}$, will be treated separately. The following treatment of Eq. (3-44) is based upon a method given by Buzbee, et. al.[16].

In general the matrix E will not be symmetric tridiagonal but a matrix D can be found that will symmetrize E through a similarity transformation $\overleftrightarrow{E} = DED^{-1}$. If D is allowed to operate on Eq. (3-44) from the left, it then takes the form

$$\overleftrightarrow{E}D\vec{\psi}_n + G_n^1 D\vec{\psi}_1 = D\vec{S}_n. \qquad (3\text{-}45)$$

It is easily shown that D has a diagonal form such that it commutes with G_n^1 as indicated.

The symmetric matrix $\overleftrightarrow{E}$ has a complete set of eigenvectors given by $\overleftrightarrow{E}\vec{\epsilon}_\alpha = \lambda_\alpha\vec{\epsilon}_\alpha$ so that the vectors $D\vec{\Psi}$ and $D\vec{S}$ can be expanded as

$$D\vec{\psi}_1 = \sum_\alpha a_{1\alpha}\vec{\psi}_\alpha \qquad (3\text{-}46)$$

$$\hat{D}s_n = \sum_{\alpha} b_{n\alpha}\hat{\psi}_{\alpha} \ . \qquad (3\text{-}47)$$

Using these expansion in Eq. (3-45), it is found that it can be rewritten as

$$[G_n^1 + \delta_n^1\lambda_{\alpha}]a_{1\alpha} = b_{n\alpha} \ . \qquad (3\text{-}48)$$

Eq. (3-48) is recognized to be a tridiagonal system in the coefficients $a_{1\alpha}$ for each index α. This equation can be solved readily by a factorization of the tridiagonal system into upper and lower off-diagonal matrices. This is a standard technique in matrix analysis, the details of which will not be given here. For an excellent presentation of this technique, the reader is referred to Ref. 17.

Once the coefficients $a_{1\alpha}$ are determined, the solution of Eq. (3-45) can be constructed using Eq. (3-46) as

$$\psi_{1g} = \sum_{\alpha} a_{1\alpha}D_g^{-1}\varepsilon_{\alpha g} \ . \qquad (3\text{-}49)$$

This is the 'intermediate' distribution function f* which has been modified for collision effects. It is noted that for the case in which the background plasma remains Maxwellian, the coefficients in Eq. (3-45) remain unchanged such that the eigenvalues and corresponding eigenvectors need be computed only once. But the construction indicated in Eq. (3-49) must be performed at every time step since the $a_{1\alpha}$ will differ as the source term (and therefore the $(b_{n\alpha})$ of Eq. (3-45) changes in time. This procedure is carried out for every zone r_i in a given time step.

Eq. (3-37) remains to be solved. This equation is actually equivalent to Eq. (3-18) i.e., the difference approximation except that the collision terms on the R.H.S. are now known as q* such that

$$\frac{f(r_i, v_g, \mu_n, t_{s+1}) - f_s}{\Delta t_s} + \frac{\mu_n \Delta v_g^4/4}{V_i \Delta v_g^3/3}\left[A_{i+1/2}f_{i+1/2} - A_{i-1/2}f_{i-1/2}\right]$$

$$+ \frac{\Delta v_g^4/4}{V_i \Delta\mu_n \Delta v_g^3/3}\left[\alpha_{n+1/2}f_{n+1/2} - \alpha_{n-1/2}f_{n-1/2}\right] = \bar{q}^* \ . \qquad (3\text{-}50)$$

Eq. (3-50) has the form of the neutron transport equation which has been differenced for S_n treatment and as such, it can be solved as in neutronica. To outline this method, note that Eq. (3-50) is an equation in five unknowns f, $f_{i+1/2}$, and $f_{n-1/2}$, can be determined from boundary conditions or from a previous time step. The other three quantities can be related by some scheme so that a system of three equations in three unknowns can be formed.

The diamond differen e relationa

$$2f = f_{n+1/2} + f_{n-1/2} \tag{3-51}$$

$$2f = f_{i+1/2} + f_{i-1/2} \tag{3-52}$$

are chosen for thia purpose. It is seen in Fig. 1 that these relations linearly interpolate between quantities defined on a topologically rectangular mesh. Using these relations in Eq. (3-50) and solving for f in terms of the known quantities $f_{n-1/2}$ and $f_{i+1/2}$ yields

$$f = \{q^*\Delta t + f_s - \frac{\Delta t \mu_n \Delta v_g^4/4}{V_i \Delta v_g^3/3}[A_{i+1/2} + A_{i-1/2}]f_{i+1/2}$$

$$+ \frac{\Delta t \Delta v_g^4/4}{V_i \Delta \mu_n \Delta v_g^3/3}[\alpha_{n+1/2} + \alpha_{n-1/2}]f_{n-1/2} \tag{3-53}$$

$$\{1 + \frac{\Delta t \Delta v_g^4/4}{V_i \Delta v_g^3/3}[\frac{1}{\Delta \mu_n}(\alpha_{n+1/2} + \alpha_{\nu-1/2}) - \mu_n(A_{i+1/2} + A_{i-1/2})]\}.$$

This equation can be used to solve for the updated distributions for all zones i, starting at the boundary of the sphere by calculating the cell centered distributions f and then extrapolating inward for the cell edged distributions $f_{i-1/2}$. Since the calculation proceeds inward toward the center of the sphere, it should only be performed for

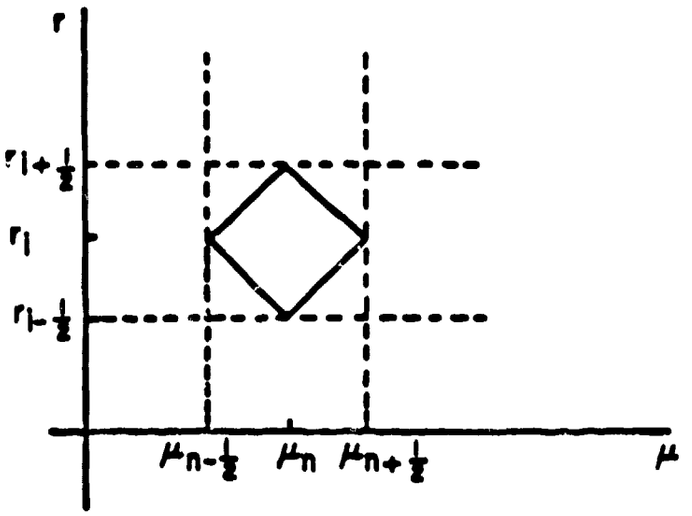

Fig. 1.--The diamond structure of the interpolating procedure shown on a partial r-μ mesh

angles directed inward to avoid the accumulation of numerical error[1] i.e., for the directions μ such that $-1 < \mu < 0$. A similar equation can be derived for outward directions by considering $f_{i+1/2}$ to be unknown and again using the diamond difference equations in conjunction with Eq. (3-50) to yield

$$f = \{q^*\Delta t + f_s + \frac{\Delta t \mu_n \Delta v_g^4/4}{V_i \Delta v_g^3/3}[A_{i+1/2} + A_{i-1/2}]f_{i-1/2}$$

$$+ \frac{\Delta t \Delta v_g^4/4}{V_i \Delta \mu_n \Delta v_g^3/3}[\alpha_{n+1/2} + \alpha_{n-1/2}]f_{n-1/2}\} \qquad (3\text{-}54)$$

$$\{1 + \frac{\Delta t \Delta v_g^4/4}{V_i \Delta v_g^3/3}[\frac{1}{\Delta \mu_n}(\alpha_{n+1/2} + \alpha_{n-1/2}) + \mu_n(A_{i+1/2} + A_{i-1/2})]\}.$$

The outward integrations can be started by using an isotropy condition at the center of the sphere which is just

$$f_{r=0,n_{outward}} = f_{r=0,n_{inward}}$$

$$n_{outward} = NN+1-n_{inward} \; . \tag{3-55}$$

This integration is done after all of the inward calculations have been performed. In this way, $f(r,v,\mu,t)$ is calculated at the updated time $t = t_{s+1}$ for all zones, speeds, and angles.

In the next section, some results obtained by this method are presented.

III. RESULTS

The calculation of the energy deposited by fast test ions as they slow down on a background plasma during the collisional transport process is typical of the benchmark problems which have evolved within the literature on charged particle transport. In a pellet plasma, for example, it is of interest to determine how this energy is distributed spatially while being partitioned to the background electrons and ions. It is also of interest to be able to determine the time history of the deposition. Some of the more important applications of these type of calculations include the treatment of fusion product transport and the analysis of injected charged particle beams. In order to demonstrate the matrix factorization (MF) method of the last sections, the transport of fusion alpha particles and beam deuterons and protons will be considered.

Before proceeding further, it is to be noted that in the transport equation, the factor Γ_{ab} has consistently been kept within the summation over the species 'b'. This is because of the dependence of Γ on the background species through the Coulomb logarithm as

$$\ln\Lambda = \ln(\lambda_d/b_o) = \ln[\lambda_d/(Z_a Z_b e^2/4\pi\varepsilon_o \mu_{ab} v^2)]. \tag{3-56}$$

In this work the arguments Λ_i and Λ_e will be approximated as

$$\Lambda_i = \frac{\lambda_d 4\pi\varepsilon_o}{Z_a Z_i e^2}\left(\frac{m_i}{m_i + m_a}\right) 2E \tag{3-57}$$

and

$$\Lambda_e = \frac{\lambda_d 4\pi\epsilon_o}{Z_a e^2} 3\theta_e \qquad (3\text{-}58)$$

which are valid approximations for cases where the electron thermal velocity $v_{e_{th}}$ is greater than the test ion velocities v, but where $v > v_{i_{th}}$. The test ion energy E in Eq. (3-57) is set to the thermal ion energy to be definite, and the Marshak correction factor[18] is applied in Eq. (3-58) when applicable.

The case of 3.5 MeV fusion product alpha parti les transporting in a spherical plasma is considered first. In this example, the background electron and hybrid D-T ion densities will be 0.2125×10^3 kg/m^3 while their temperatures are taken to be equal at 50 keV. Although here the temperatures are set equal, the code does allow for different electron and ion temperatures.

It is chosen to compare the results of the MF calculations with those given by Mehlhorn and Duderstadt in Ref. 9 since their method also allows for velocity space dispersion. In order to match the zoning used in their modified neutronics code TIMEX-FP, 13 radial zones are used while the velocity space variables are discretized by 4 μ directions and an 18 point speed grid. The zone width is taken to be $.7742 \times 10^{-2}$ m which is equivalent to $.035\lambda_s$ where λ_s is the range of alpha particles on electrons at the density and temperature given above. Further, in this problem, the arguments of the Coulomb logarithm are not calculated by Eqs. (3-57) and (3-58) but the values of $\ln\Lambda$ are set as $\ln\Lambda_e = 8.25$ and $\ln\Lambda_i = 18.56$ as they were in Ref. 9. The details of the energy deposition calculation are given in In Figures 2 and 3, the fraction E_d/E_o of the initial alphaparticle energy E_o deposited per zone to the background electrons and ions, respectively, is plotted for each zone. It can be seen that the MF method yields results which are in very good agreement with those reported in Ref. 9. In both Figures 2 and 3, the peaks of the spatial deposition profiles occur in the same zones and are nearly identical in magnitude. Similarly, the stopping lengths calculated by the MF method enjoy close agreement to those previously reported. Although small differences occur in the two methods' calculations of the amount of energy deposited in the first few zones to both electrons and ions, the results of the MF method should be reliable since it does not seem to encounter the difficulties near localized sources that the S_n techniques used in TIMEX-FP might.

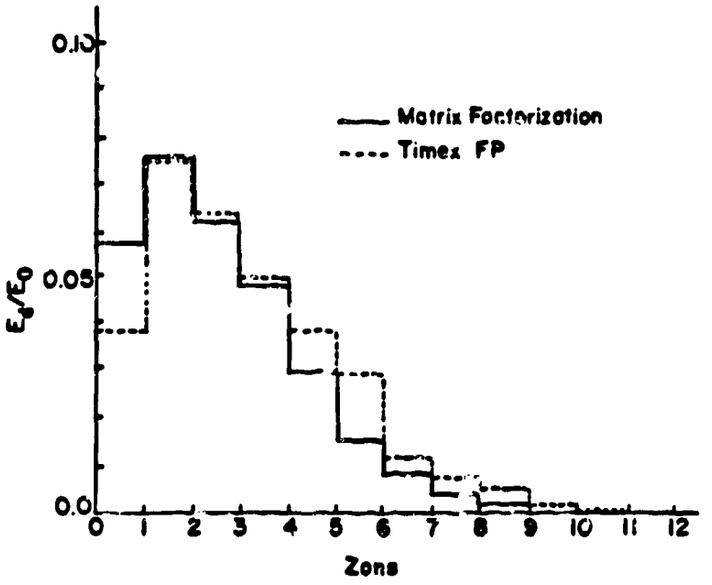

Fig. 2.--Fraction of initial alpha particle energy deposited per zone to electrons

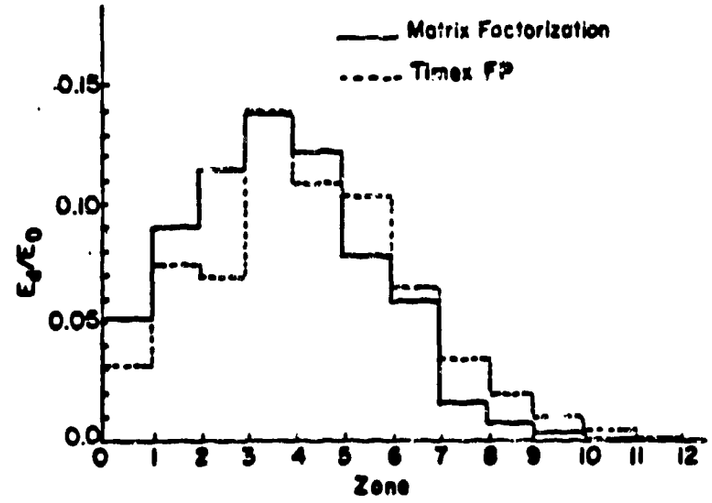

Fig. 3.--Fraction of initial alpha particle energy deposited per zone to ions

In order to study the effects of the diapersion in velocity space which the alpha particles undergo as they scatter on the plasma, the number of angles NN, used in the calculations was varied. In Figures 4 and 5 the spatial deposition profiles are again given for electrons and ions separately. It is seen that by increasing the number of directions in which the alpha particle distribution function can be defined, for the case of deposition to electrons, the spatial profile's peak is decreased while deposition to the outer zones is increased. In the case of the ions, the peak is also diminished but shifted to the right with the deposition to the outer zones again increasing. This behavior is to be expected for the following reasons. Since the initially isotropic alpha particles are at higher energies than the background electrons and ions, their distribution will depart from the isotropic form as they scatter in an attempt to reach a thermal equilibrium. Although the alpha energy may diminish after the first few collisions in zones near the center of the sphere, the energy is more directed in the outward directions in these zones. They will approach a thermal equilibrium after enough collisions have occurred along their path, so that their distribution will again acquire an isotropic character in the outer zones of the mesh. At this time the particles will have no preferred direction, so that the amount of backscattering will become the same as the amount of forward scattering, thus resulting in higher deposition to these outer zones. That this behavior is indeed the case, is established by following the distribution of the cosine (μ)

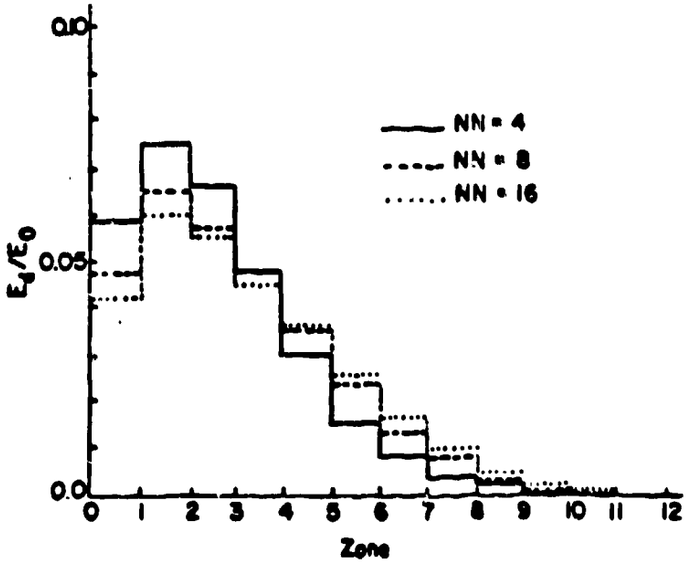

Fig. 4.--Fractional deposition per zone to electrons for an increasing number of directions (NN)

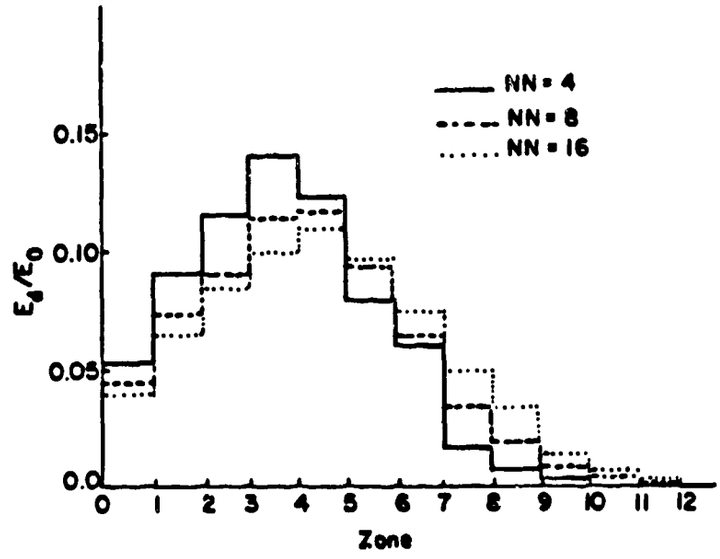

Fig. 5.--Fractional deposition per zone to ions for for an increasing number of directions (nn)

of the alpha particles' velocity vectors with respect to the radial vector as a function of time. In Figure 6 this spectral information is shown for the center zone at t = 0 while the curves at other times are appropriate to the third zone on the mesh. It is seen that the distribution (normalized to unity on the abscissa) becomes peaked toward a positive cosine almost instantaneously, showing that the alpha energy is highly directed toward the outer zones. As time (NT) progresses, the particles scatter and lose their energy and the distribution tends toward a Maxwellian at the background temperature. From this information, it can be concluded that by using too few angles in this type of calculation, the results may become biased in showing too much deposition in the first few zones and in ignoring the backscattering effects in the outer zones.

It is interesting to note that the plots in Figure 6 contain data points which appear jagg This is due to the use of a large time step in the algorithm, wh n gives rise to small fluctuations in the distribution information, a common occurrence in some finite difference schemes. Although this phenomenon could be detrimental in some algorithms, the MF method remained absolutely conservative and convergent.

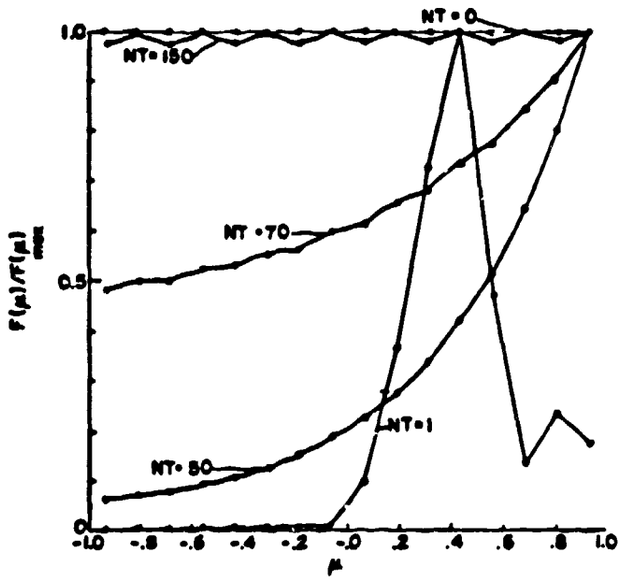

Fig. 6.--Angular spectra of the distribution function at the 3rd position on the zone grid. At the first time step (NT), the spectra is shown for the first zone

In Figure 7 the time dependent energy deposition history is shown for both deposition on electrons and on ions. As a check on the accuracy of this method, the curve showing the total energy fraction deposited to both ions and electrons was calculated using the appropriate moment of the L.H.S. of the transport equation, Eq. (3-18). It can be seen that the code remained energy conserving.

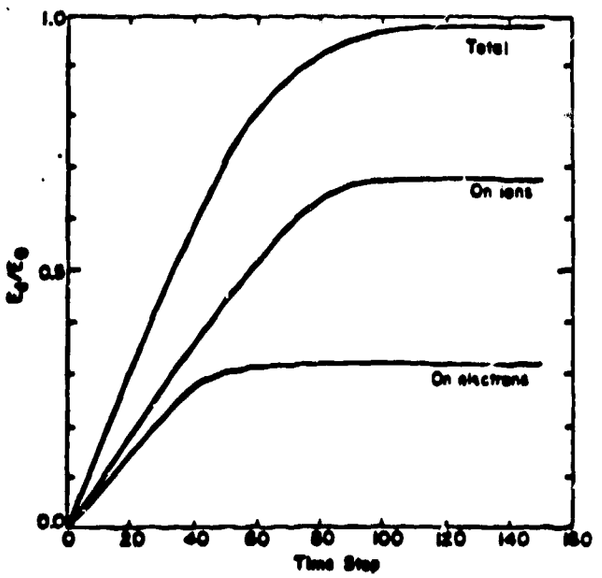

Fig. 7.--Time history of deposition to both electrons and ions

The efficiency for the MF method is demonstrated in Figures 8 and 9. The same computations described above for four angles, 13 zones and 18 velocity grid points were performed using 150 time steps (NT) at a

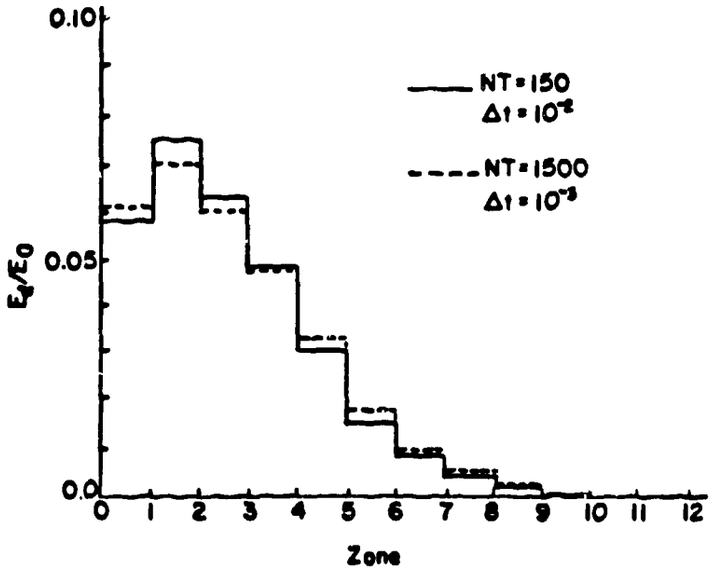

Fig. 8.--Fractional deposition per zone to electrons for two time step sizes and the corresponding number of iterations

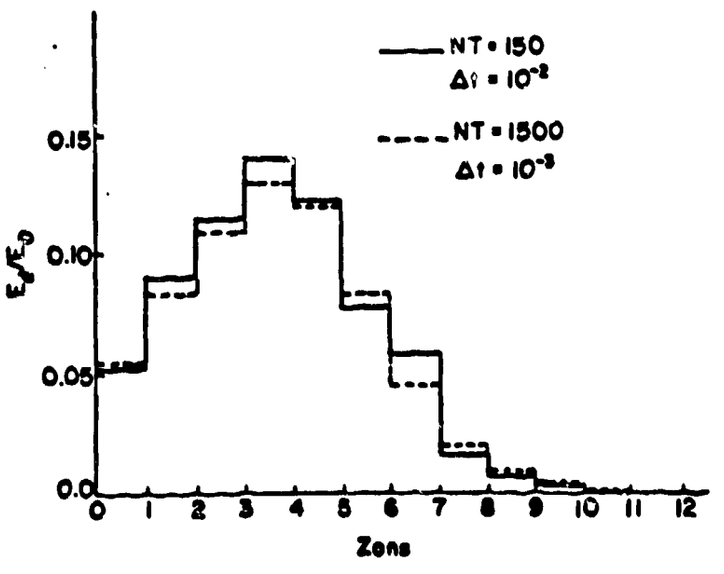

Fig. 9.--Fractional deposition per zone to ions for two time step sizes and the corresponding number of iterations

time increment of .01 and then carried out again using 1500 time steps at $\Delta t = .001$. Here the time increment Δt is scaled to the slowing-down time of alpha particles due to electrons at 50 keV which is equal to 8.47×10^{-3} sec. It can be seen that very little accuracy is lost by using the larger time step. The calculation using 150 time steps required 5 seconds of CPU time on the CRAY I computer.

It is noted that the total deposition fraction in time tends towards unity but becomes asymptotic at a value less than unity. This is, of course, due to the fact that the alpha particle does not lose all of its kinetic energy but only slows down to an energy defined by the temperature at thermal equilibrium.

The energy deposited to a plasma by an injected beam can be calculated by introducing a distribution function characterizing the beam at the outermost zone of the system. In the examples which follow, the zoning used in the previous examples is retained but a delta function distribution (in speed) defined at one ingoing angle is used to simulate a beam entering at the boundary.

In the first example, a beam of 1 MeV deuterons impinging on D-T plasma (at the same temperature and density as before) at the outermost zone (zone 13) is considered. The delta function is defined at their velocity corresponding to that energy which is $v = 9.823 \times 10^6$ m/sec. In Figures 10 and 11, the deposition profiles are shown for the case in which the beam consists of an initial burst of ingoing deuterons. Since the beam velocity is much less than the electron thermal velocity in this case, the deuterons should tend to deposit their energy on the background ions in greater proportion. This is seen to be the case.

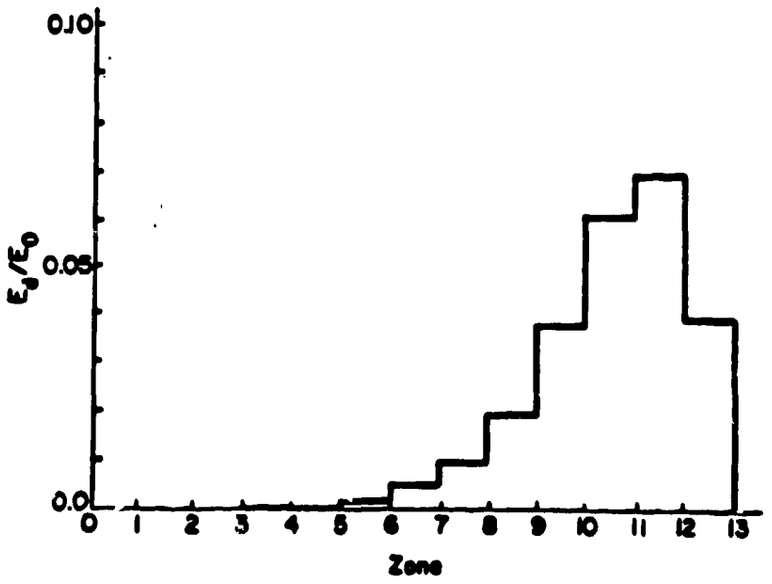

Fig. 10.--Fraction of initial deuteron energy deposited per zone to electrons for a beam entering at zone 13

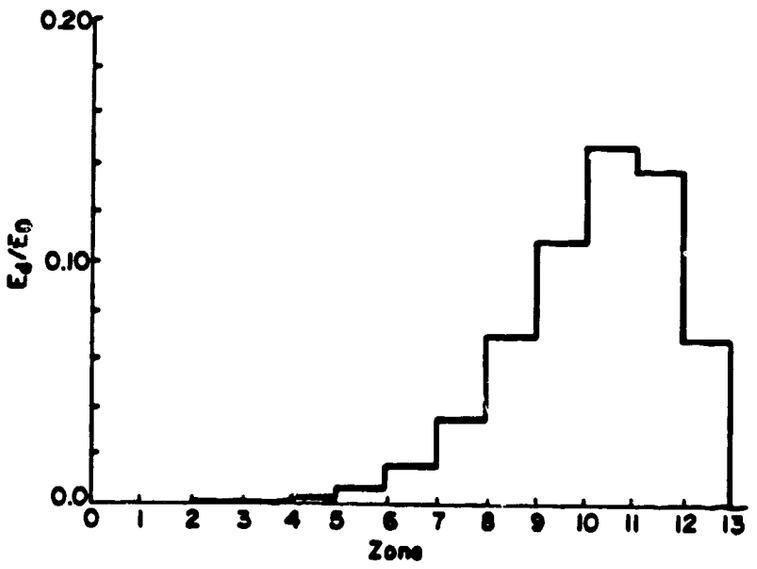

Fig. 11.--Fraction of initial deuteron energy deposited per zone to ions for a beam entering at zone 13

In Figures 12 and 13, the deposition profiles are shown for an initial burst of 500 keV ingoing protons. Since the proton velocity is the same as above ($v = 9.823 \times 10^6$ m/sec) the same tendency to deposit more energy to the ions should be observed. In addition though, since the mass of the protons is less than that of deuterons, they are more easily deflected and so should deposit their energy much more quickly i.e., within the first few zones. Again, this behavior is verified in the figures. Both of the above calculations required about 4.5 seconds of CPU time on the CRAY I.

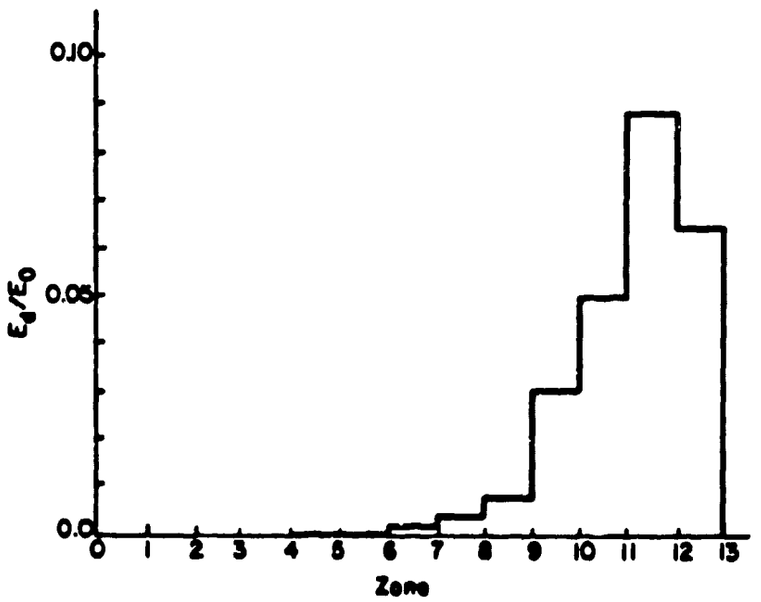

Fig. 12.--Fraction of initial proton energy deposited per zone to electrons for a beam entering at zone 13

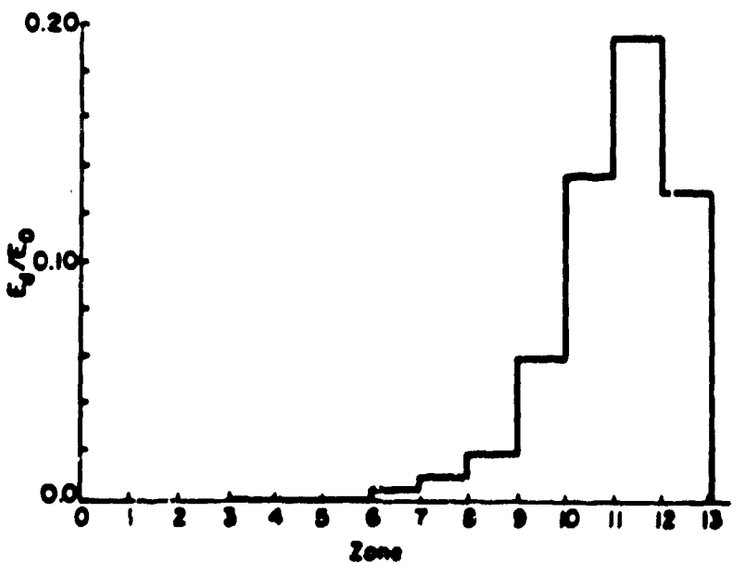

Fig. 13.--Fraction of initial proton energy deposited per zone to ions for a beam entering at zone 13

REFERENCES

1 G.I. Bell and S. Glasstone, "Nuclear Reactor Theory", Van Nostrand Reinhold, New York, 1970.

2 J.J. Duderstadt and W.R. Martin, "Transport Theory", John Wiley and Sons, New York, 1979.

3 J. Killeen and K.D. Marx, "Methods of Computational Physics", Vol. 9, Academic Press, New York, 1969.

4 J. Killeen, A.A. Mirin, and M.E. Rensink, "Methods of Computational Physics", Vol. 16, Academic Press, New York, 1976.

5 P.A. Haldy and J. Ligou, Nucl. Fusion 17 (1977), 1225.

6 E.G. Corman, W.E. Loewe, G.E. Cooper and A.M. Winslow, Nucl. Fusion 15 (1975), 377.

7 M.J. Antal and C. Lee, J. of Comp. Phys. 20 (1976), 298; M.J. Antal and C. Lee, Nucl. Sci. Eng. 64 (1977), 379.

8 P.A. Haldy and J. Ligou, Nucl. Sci. Eng. 74 (1980), 178.

9 T.A. Mehlhorn and J.J. Duderstadt, J. of Comp. Phys. 38 (1980), 86; T.A. Mehlhorn, Ph.D. dissertation (The University of Michigan, 1978)

10 J.E. Morel, personal communication, Sandia Laboratories (1979).

11 A. Andrade, T.A. Oliphant, and J. Kammash, J. of Comp. Phys. 42 (1981), 367.

12 A. Andrade, "Numerical Solutions of the Fokker-Planck Charged Particle Transport Equation", Los Alamos report LA-8985-T (September, 1981)

13 M.N. Rosenbluth, W.M. MacDonald, and D.L. Judd, Phys. Rev. 107 (1957), 1.

14 B.G. Carlson and K.D. Lathrop in "Computing Methods in Reactor Physics", H. Greenspan, C.N. Kelber, and D. Okrent, eds., Gordon and Breach, New York, 1968.

15 J.S. Chang and G. Cooper, J. of Comp. Phys. 6 (1970), 1.

16 B.L. Buzbee, G.H. Golub, and C.W. Nielson, SIAM J. Numer. Anal. 7, 4 (1970), 637.

17 E. Isaacson and H.B. Keller, "Analysis of Numerical Methods", John Wiley and Sons, New York, 1966.

18 L. Spitzer, Jr., "Physics of Fully Ionized Gases", Interscience, New York, 1962.